# High-frequency Vibration in Flagellar Axonemes with Amplitudes Reflecting the Size of Tubulin

**Shinji Kamimura and Ritsu Kamiya***

College of Arts and Sciences, the University of Tokyo, Meguro-ku, Tokyo 153, Japan; and *Department of Molecular Biology, School of Science, Nagoya University, Nagoya 464-01, Japan

***Abstract.*** Flagellar axonemes of sea urchin sperm display high-frequency (~300 Hz) vibration with nanometer-scale amplitudes in the presence of ATP (Kamimura, S., and R. Kamiya. 1989. *Nature (Lond.).* 340: 476–478). The vibration appears to represent normal mechanochemical interaction between dynein and microtubules because the dependence of the frequency on MgATP concentration is similar to that of the axonemal motility, and because it is inhibited by micromolar concentrations of vanadate. In this study a two-dimensional photo-sensor was used to characterize this phenomenon in detail. Several new features were revealed. First, the vibration was found to be due to a back-and-forth movement of the doublet microtubules along the axonemal length. Two beads attached to different parts of the same axoneme vibrated in unison, i.e., synchronized exactly in phase. This suggested that the outer doublet can be regarded as a stiff rod in vibrating axonemes. Second, evidence was obtained that the amplitude of the vibration reflected the number of active dynein arms. Third, under certain conditions, the vibration amplitude took stepwise values of $8 \times N + 4$ nm ($N = 0, 1, 2, 3,$ or 4), indicating that the amplitude of microtubule sliding was limited by the size of tubulin dimer (8 nm) or monomer (4 nm). To explain this phenomenon, a model is presented based on an assumption that the force production by dynein is turned off when dynein is subjected to tensile force; i.e., dynein is assumed to be equipped with a feedback mechanism necessary for oscillation.

THE beating of cilia and flagella is a result of interdoublet sliding driven by dynein arms (Gibbons, 1981). The oscillatory movement of an axoneme with a regular waveform must be produced by controlled activation and inactivation of specific dynein arms, but the mechanism for this control has been unknown. Currently prevailing theories postulate that the activity of dynein arms is controlled by the mechanical state of axoneme, such as curvature, which in turn is determined by the activity of dynein arms; axonemes oscillate because of this feedback (Brokaw, 1985). However, it remains possible that dynein arms have an intrinsic tendency to oscillate, and this nature of dynein somehow gives rise to the beating movement of the axoneme (Brokaw, 1990).

By using an optical device that can detect one-dimensional subnanometer displacements of polystyrene beads, we have recently found a novel phenomenon that appears to be important when considering the mechanism of axonemal motility: an ATP-dependent nanometer-scale vibration in fragmented axonemes at frequencies as high as 300 Hz (Kamimura and Kamiya, 1989). The vibration frequency depended on the MgATP concentration in a manner consistent with Michaelis-Menten kinetics. The Km value was similar to those obtained from the ATP dependence of the best frequency of reactivated axonemes (Brokaw, 1967; Gibbons and Gibbons, 1972; Gibbons et al., 1982) and of the microtubule sliding velocity in disintegrating axonemes (Yano and Miki-Noumura, 1980; Takahashi et al., 1982). Vanadate, a potent inhibitor of the dynein ATPase (Gibbons et al., 1978, 1985; Kobayashi et al., 1978), blocked the vibration completely at micromolar concentrations. These observations indicate that the high-frequency axonemal vibration is closely related to the function of dynein, although the molecular mechanism that produces such a vibration is unknown.

Since the high frequency vibration has amplitudes on the order of the size of tubulin and dynein, we may expect that analyses of it will provide information about the elementary process of force production by these molecules. Thus we examined this phenomenon in detail using an improved analogue photo-sensor that can detect nanometer-scale displacements in two dimensions. We also analyzed the effects of dynein inhibitors. Our study not only refined the previous observations, but also revealed several novel features. In particular, under certain conditions, the vibration amplitude was found to have discrete stepwise values that reflected the size of tubulin.

## Materials and Methods

### Axoneme Samples

Spawning of male sea urchin (*Hemicentrotus pulcherrimus* or *Anthocidaris*

*crassispina*) was induced with 0.5 M KCl. Dry sperm was collected and kept refrigerated until use.

The procedure for demembranation was as described (Gibbons and Gibbons, 1972). Briefly, 5 μl of dry sperm was diluted with 50 μl of natural sea water, and then added to 200 μl of demembranating medium (0.04% [wt/vol] Triton X-100, 150 mM KCl, 2 mM $MgSO_4$, 1 mM EDTA, and 1 mM DTT and 10 mM Tris-HCl, pH 8.0, 4°C). After being swirled gently for 30–60 s, the suspension of demembranated spermatozoa was diluted to ~1,000 μl with a standard buffer solution containing 20 mM Tris-HCl (pH 8.0), 200 mM K-acetate, 2 mM $MgSO_4$, 0.5 mM EGTA, 0.1 mM EDTA, and 1 mM DTT. This diluted suspension was used as the sample of flagellar axonemes.

## Chemicals

ATP was purchased from Boehringer, Mannheim, Germany. Polystyrene microbeads of carboxylated type (diameter 0.9 μm, no. 8226) and amino type (diameter 1.12 μm, no. 17010) were from Polyscience Co., Warrington, PA.

## Microscope and Specimen

A Nikon Optiphoto phase-contrast microscope with a reverse-contrast objective (Plan ApoDF ×100, NA 1.4, Nikon-Engineering, Tokyo, Japan; or SPlan ×100NH, NA 1.25, Olympus, Tokyo, Japan) was used for detection of the nanometer-scale vibration. The light source was a 150 W tungsten-halogen lamp powered by stabilized DC. The microscope specimen stage was specially designed so that its position can be electrically controlled in x- and y-directions by means of a pair of linear actuators driven by servo DC motors (LA-30-10-C; Harmonic Drive Systems, Tokyo, Japan) and a pair of piezoelectric actuators (PSt 1000/5/5; Dr. Lutz Pickelmann, Munich, Germany). The microscope was placed on an air-damping table (Meiritsu-Seiki, Tokyo, Japan) (Fig. 1 *A*).

For observation of microbeads attached to the flagellar axonemes, the suspension of demembranated sperm was first introduced into the space between a glass slide and a cover slip held ~0.8 mm apart with a pair of cover slip strips (No. 0 thickness). After standing for 2–3 min, the sample chamber was perfused with the standard buffer solution to wash out the flagellar axonemes that were not attached to the glass surface. Microbeads were then attached to the axonemes stuck to the glass surface by perfusion with 0.025% (wt/vol) suspension in the standard buffer. When the microbead suspension permeated the entire area of the perfusion chamber the sample was kept standing for 2–3 min. During this time some fraction of the beads became attached to the axoneme. Free microbeads were washed out by perfusion with buffer. The high frequency vibration was then induced by perfusing the sample chamber with buffer solutions containing appropriate concentrations of ATP. Usually the vibration was observed in 1/5 to 1/3 of the total microbeads attached to the axoneme. Because the vibration stably lasted for more than 30 min, we were able to take data on a single microbead while successively changing solution conditions by repeated perfusion.

To attach axonemes to the glass surface firmly, cover slips were coated with poly-L-lysine (mean mol wt >300,000, no. P-1024; Sigma Chemical Co.); a surface was placed on 0.02% aqueous solution, washed, wiped, and dried in the air.

## Analogue Sensor for Two-dimensional Measurement

The photo-detector used to measure the displacement of microbeads was essentially based on the one reported previously (Kamimura, 1987; Kamimura and Kamiya, 1989). An important difference is that the new device detects two-dimensional displacements rather than one-dimensional ones.

The magnified image of a microbead was projected onto a quadrant-type photodiode (model S1557; Hamamatsu Photonics, Hamamatsu, Japan) placed on the back focal plane of the microscope. The photo-sensing area of the quadrant photodiode was 1.0 mm in diameter. The final magnification of the image on the diode was 780×.

The intensity of the light coming into each quadrant area (a–d) was measured separately with four current-voltage converters (model OPA111-CM; Burr-Brown, Tucson, Arizona). Feedback resistors of 2 G ohm were used. The amplifier (Fig. 1 *B*) yielded two output signals, (a + b) − (c + d) and (a + d) − (b + c), corresponding to the displacements in x- and y-directions, respectively. The output signals were fed into an active low-pass filter (cut-off frequency = 1 kHz) to reduce noise. The output was linear with the displacement of the microbead as long as the magnified image was positioned near the center of the photo-sensing area. The magnitude of the measurable displacement was typically ~500 nm, which depended on the size of the microbead.

Throughout the present study we selected axonemes whose longitudinal axes were oriented in the x-direction of the two-dimensional sensor. This direction was determined by the flow, with which the axonemes tended to be oriented. Thus, the x- and y-outputs of the sensor in the present study represent the displacement in the longitudinal and lateral directions of an axoneme. To determine whether the motions of two microbeads attached to the same axoneme are correlated with each other, we analyzed the auto- and cross-correlation functions between their movements. In such cases the microscope image was split into two by a half mirror, and the motions of the two microbeads were independently analyzed with two photo-sensing apparatuses (Fig. 1 *A*).

## Calibration of the Output

Calibration of the output against known amounts of displacement was first carried out using a pinhole of 1 μm diameter. The pinhole was placed under a 20× objective (SPlan, Olympus) and observed with conventional bright-field illumination. A magnified image (141×) of the pinhole was projected onto the photodiode sensor as in the case of microbeads. The output voltage from the sensor was recorded after the sensor was displaced by a micrometer screw by various lengths in a 30–60-μm range. The output was almost linearly related to the displacement of the sensor as described previously (Kamimura, 1987), and from this relationship we calibrated the output against unit displacement of the sensor (mV/μm). Dividing it by the magnification of the pinhole image yielded the sensor output per unit displacement of the pinhole (mV/nm). Next, the microscope stage was displaced in a nanometer range by a piezoelectric actuator driven by square pulses of a known voltage. From the output and the previous calibration (mV/nm) we determined how much the piezoelectric actuator displaced the stage on which the pinhole was placed. It was usually 12–15 nm/V varying somewhat with the mechanical adjustment of the friction of stage. This calibration was carried out before and after a series of experiments. To determine the sensitivity of the optical sensor in actual measurement with microbeads, pulses of a known voltage (0.5–1 V) were applied to the piezoelectric actuator during the measurement. Since we knew how much displacement was caused by the actuator at a given applied voltage, we were able to determine the amount of displacement from the output.

## Data Analysis

Both x- and y-outputs were introduced into a computer (PC9801RX; NEC, Tokyo, Japan) through an analogue-digital converter (ADX-98; Canopus Electronics, Kobe, Japan) and analyzed with a fast-Fourier-transform (FFT) program (Signas, Canopus Electronics). The sampling rate of the analogue-digital converter was 2–50 kHz. The outputs of the sensor were also recorded with a digital-audio-tape (DAT) recorder (500ES; SONY, Tokyo, Japan) for further analyses.

Correlation between x- and y-outputs of the sensor was calculated using data sampled at 50 kHz for 20.48 ms (1,024 points). Auto- or crosscorrelation functions were averaged from calculations with ten different sets of such data.

For the analysis of the amplitude distribution in the output of the sensor, a computer program was written to detect the peak value. A peak maximum was defined as a point before and after which the output decreased or increased monotonically for at least six data points (corresponding to 0.6 ms).

# Results

## Precision Measurement of Microbead Motion in Two Dimensions

As we have described in the previous study using a one-dimensional sensor (Kamimura and Kamiya, 1989), the differential output from a pair of photodiodes can detect a displacement of a microbead with a spatial resolution better than a nanometer and a time resolution of ~1 ms. The most important factor that determined the spatial resolution was mechanical noise.

Fig. 2 shows the amplitude and frequency distribution of noise present in our system in three cases: (*a*) no light was introduced into the sensor (Fig. 2, *A* and *B*); (*b*) only the

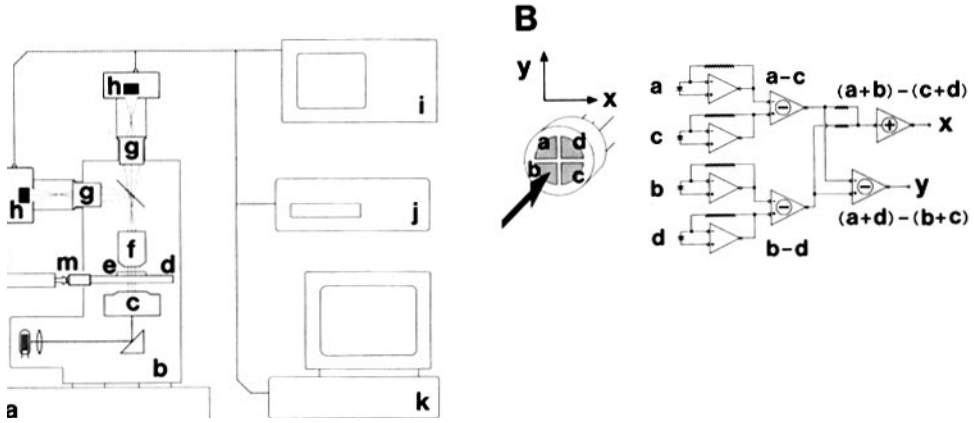


*Figure 1.* Diagram (*A*) and circuit (*B*) of the apparatus. (*A*) (*a*) Air damping table; (*b*) phase-contrast microscope; (*c*) condenser lens; (*d*) micromanipulating stage; (*e*) glass slide; (*f*) objective; (*g*) ocular; (*h*) two-dimensional sensor; (*i*) oscilloscope; (*j*) digital-audio-tape (DAT) recorder; (*k*) microcomputer with an analog-digital converter; (*l*) linear actuator driven by a servo-DC-motor; (*m*) linear actuator driven by a piezoelectric element. The motion of the micromanipulating stage was controlled by external signals in both x- and y-directions. The half mirror which splits the light path into upward and lateral directions was used only when motions of two different microbeads were recorded at the same time in order to analyze cross-correlation. (*B*) Schematic diagram of the circuit for the two-dimensional detector. The light input into each quadrant area of the photodiode was separately measured with four current-voltage converters (OPA111-CM, Burr-Brown) with feedback resistances of 2 Giga-ohm. Displacements in x- and y-directions were respectively obtained from $(a + b) - (c + d)$ and $(a + d) - (b + c)$, which were computed by analog amplifiers.

background light of the microscope image was projected on the sensor (Fig. 2, *C* and *D*); and (*c*) an image of a microbead attached to the glass surface was projected on the sensor (Fig. 2, *E* and *F*). Fig. 2, *A* and *B* represent pure electronic noise. Fig. 2, *C* and *D* show, in addition to the electronic noise of the amplifier, the noise derived from the statistical fluctuation of the light source (photon noise) or from that of the current through the photodiode (shot noise). In addition to these sources of noise, Fig. 2, *E* and *F* must also involve noise caused by fluctuation of the position of the microbead image with respect to the sensor due to mechanical vibration of the total system. Compared with the first two cases, a significant level of noise was apparent in Fig. 2, *E* and *F*. The noise appearing as several peaks around 200 Hz was difficult to eliminate. However, we could distinguish it from the axonemal vibration in FFT spectra because the mechanical noise displayed characteristic sharp peaks at constant frequencies with amplitudes <1 nm. The magnitude of the mechanical noise varied from one experiment to another. The exact reason for this variation is unknown, but it is likely that the vibration of laboratory building is the most important factor. Because of these noises, the precision with which our apparatus can measure the microbead displacement was limited to 0.5–2 nm. In averaged FFT spectra, however, displacements as small as the level of shot noise, i.e., ~0.05 nm, can be detected if the movements repeat at a constant frequency.

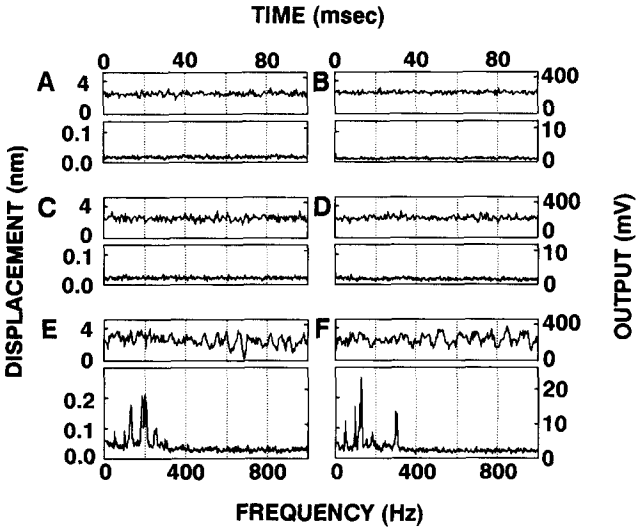


*Figure 2.* Noise appearing in the apparatus. The x- and y-outputs are shown in the left (*A*, *C*, and *E*) and right figures (*B*, *D*, and *F*). (*A* and *B*) Noise observed when no light was introduced into the sensor. (*Upper figures*) Time-domain recordings of the noise sampled at 2 kHz. Time scale is shown in the upper abscissa (full scale = 100 ms). The vertical scales in mV and nm are as shown in the right and the left ordinates, respectively. (*Lower figures*) FFT spectra from the output. The spectra shown are average from 10 samplings (2 kHz, 1,024 point each). Horizontal scale is shown in the lower abscissa (full scale, 1,000 Hz); vertical scales in mV and nm are shown on the right and left ordinates. (*C* and *D*) Noise observed when only the background light of the microscope image was put into the photosensor. The arrangement of figures is as above. (*E* and *F*) Noise observed when a microbead attached on the glass surface was used for measurement.

### *Movements of Microbeads Attached to Reactivated Axonemes*

Microbeads attached to the axonemes of sea urchin sperm flagella displayed a regular vibration in the presence of ATP as has been described in our previous report (Kamimura and Kamiya, 1989). In the previous study we used axoneme fragments detached from sperm heads, because we wanted to examine axonemes lacking the ability to beat. We found, however, that essentially identical results could be obtained with axonemes of intact length, attached to sperm heads, provided that they adhered to the glass surface and did not beat. Hence, in this study, we used demembranated sperm without fragmenting them.

The vibration frequency depended on the ATP concentration in a manner consistent with Michaelis-Menten kinetics, as observed before (Kamimura and Kamiya, 1989). The apparent Km value and the maximal frequency measured with six axonemes were within ranges of 0.06–0.11 mM MgATP

and 330–430 Hz (at 21–25°C), respectively. These values agreed with those in the previous study. It should be noted that although the ATP concentration affected the vibration frequency, it had only a minor difference on the amplitude of the vibration (see Kamimura and Kamiya, 1989, for example).

The records of vibration indicated that the movement of a bead can be regarded as regular vibration superimposed on a random motion (see below). When ATP was depleted, the amplitude of the random motion decreased in the x-direction parallel to the axoneme axis, as well as in the y-direction perpendicular to it (data not shown). The depletion of ATP thus increased the stiffness of the axoneme, in agreement with previous reports (Gibbons and Gibbons, 1974; Okuno and Hiramoto, 1979). The ATP-depleted axoneme vibrated again when 1 mM ATP was introduced.

### *Effects of Inhibitors*

The high frequency vibration was inhibited by drugs known to inhibit axonemal motility. Fig. 3 shows the effect of vanadate, a potent inhibitor of dynein ATPase. The effect of vanadate resembles that of lowered ATP concentrations in that both decrease the rate of ATP hydrolysis, but their effects on the high frequency vibration differed strikingly. Unlike low ATP concentrations, up to 1 $\mu$M of vanadate reduced the peak height in the FFT spectra with little effects on the vibration frequency. The decrease in the peak height in the FFT spectra was mostly due to the decrease in the amplitude of individual vibration, although the waveform became somewhat irregular at higher vanadate concentrations. In this particular example, the peak-to-peak amplitude of vibration was typically ~7 nm in the absence of vanadate (Fig. 3 A, *upper figure*), while it decreased to ~2 nm in the presence of 1 $\mu$M vanadate (Fig. 3 *C*, *upper figure*).

N-ethylmaleimide (NEM),[1] a thiol agent, is also known to be a potent blocker of the ATP hydrolysis by dynein (Shimizu and Kimura, 1974). We found that the effect of NEM was similar to that of vanadate; it reduced the vibration amplitude, but not frequency, in a time-dependent manner. Although brief NEM treatment of axoneme is known to increase its ATPase rate (Shimizu and Kimura, 1974), no increase in vibration frequency or amplitude was observed.

### *Direction of Vibration in Axonemes Firmly Attached to a Glass Surface*

For an understanding of the mechanism of the high frequency vibration, it is important to determine the direction of vibration. For this purpose we monitored the movement of microbeads in the x- and y-directions simultaneously. With usual specimens, however, it was not easy to tell in which direction the vibration actually occurred, because the amplitude of random Brownian motion was greater than that of the regular motion. Furthermore, although many beads tended to vibrate regularly only in the x-direction (parallel to the axoneme axis) as shown in Fig. 4 *A*, some displayed regular vibration in both x- and y-directions (Fig. 4 *B*). Random movements were usually more pronounced in y-direction than in x-direction, resulting in a trajectory of the movement elongated in y-direction (the rightmost figure in Fig. 4, *A* and *B*).

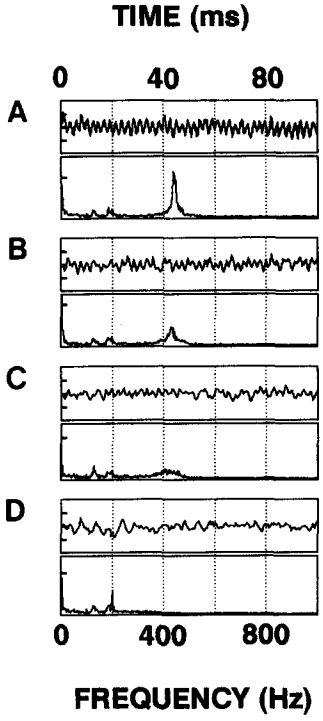


*Figure 3.* Effect of vanadate on the axonemal vibration. The axoneme examined was firmly attached to the glass surface which had been coated with poly-lysine. The concentrations of vanadate are (*A*) 0, (*B*) 0.5, (*C*) 1.0, and (*D*) 2.0 $\mu$M. ATP concentration: 1 mM. Outputs for x-direction and their averaged spectra are shown as in Fig. 2. Note that the amplitude decreased concomitantly with the increase in the vanadate concentration while the peak frequency was kept almost constant until the vibration almost vanished (*D*). The vertical scales are in 5 (outputs) and 1 nm (FFT spectra). Sample: *Anthocidaris crassispina*. Temperature: 28°C.

The large random movement appeared to result from loose attachment of axonemes to the glass surface. We therefore coated the cover slips with poly-lysine to make the attachment firmer, and found that such a treatment actually suppressed the random movements. After the poly-lysine coating of the glass, fewer microbeads (<10% of the total microbeads attached to axonemes) showed active vibration, although more axonemes became attached to the glass. In those small numbers of microbeads that still displayed active vibration, the movement was observed to occur predominantly in the x-direction. Fig. 4, *C* and *D* show two such cases, where random motion in the y-direction was reduced almost to the noise level of the equipment while the regular vibration in the x-direction clearly persisted. Unlike the vibration observed without the poly-lysine coat, the vibration observed in these firmly attached axonemes sometimes (~40%) displayed nonsinusoidal waveforms, with amplitudes significantly larger than those observed without the poly-lysine coat (Fig. 4 *D*; see below). It was, however, always evident that the vibration occurred predominantly in the x-direction in these experiments.

### *Correlation of Motion between two Microbeads on an Axoneme*

To confirm the above conclusion that the vibration occurs predominantly in the x-direction, we analyzed the cross-correlation of motion between different microbeads attached to the same axoneme (e.g., microbeads I, II and III in Fig. 5). In this experiment, poly-lysine was not used because we wanted to eliminate the possibility that we may artificially create a directionality.

When a microbead vibrates with a constant frequency, the autocorrelation function of its position will show a periodic wave with peaks at times 0, $p$, $2p$, $3p$, . . . , where $p$ is the

1. *Abbreviation used in this paper*: NEM, N-ethylmaleimide.

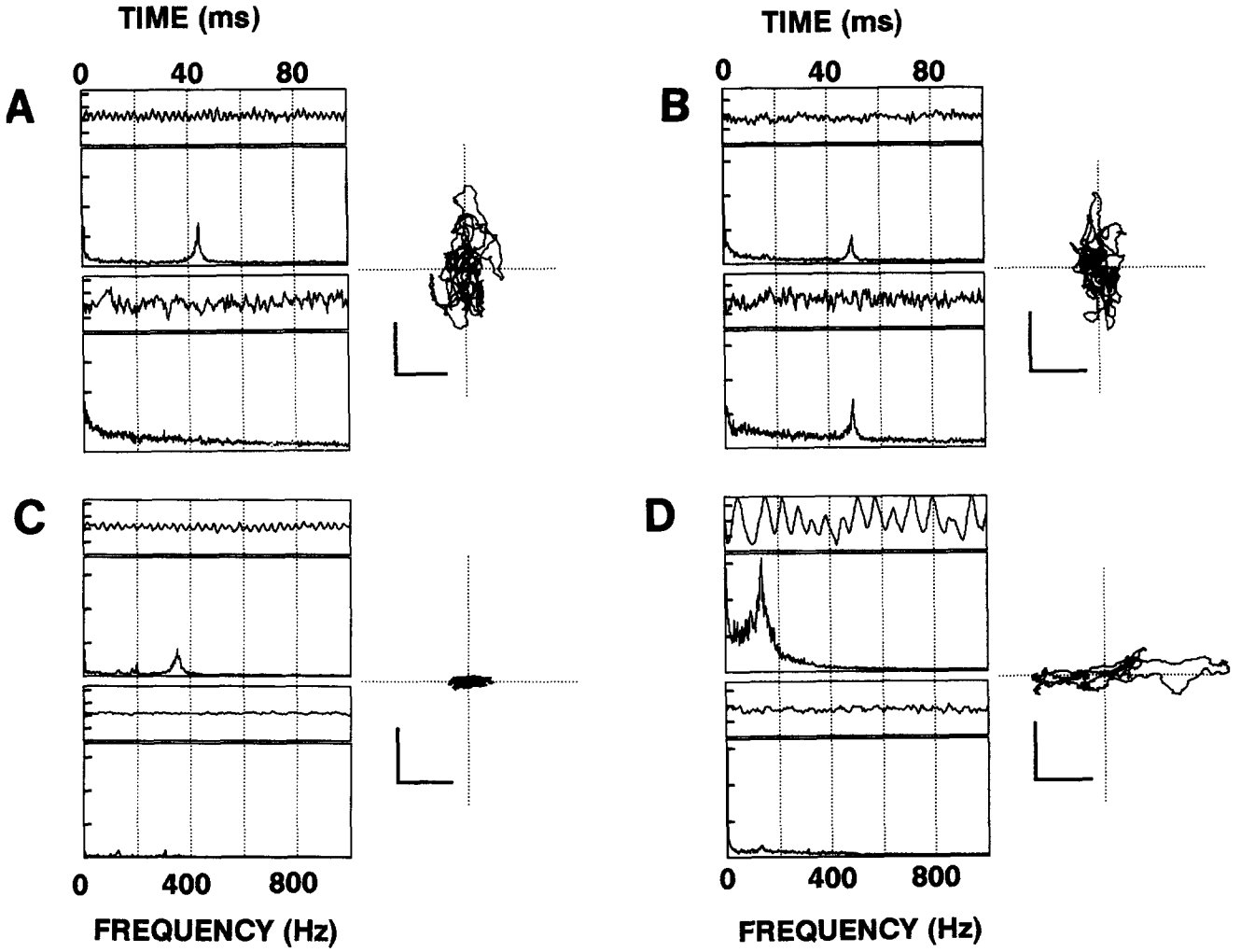


*Figure 4.* Four examples of the axonemal vibration at 1 mM ATP, showing the movements in x-direction (parallel to the axoneme axis) and y-direction (perpendicular to the axoneme axis). Cover slips were either not coated (*A* and *B*) or coated with poly-lysine (*C* and *D*). On the left side of each figure, direct outputs and averaged FFT spectra for the motion in x-direction (*upper figures*) and y-direction (*lower figures*) are shown. The vertical scales are in 10 nm (outputs) and 1 nm (FFT spectra). The trace on the right side is a two-dimensional trajectory of the vibrating bead. (*A*) A case when little noise was present. Regular vibration occurred only in the x-direction. (*B*) An example that showed peaks in the FFT spectra from the y-signal as well as those from the x-signal. (*C*) An example of regular and sinusoidal vibration, with amplitudes of ~4 nm. (*D*) An example that showed a somewhat chaotic pattern with amplitudes of 10–30 nm. For its amplitude, see Fig. 8. Note that, in *C* and *D*, the vibration occurred mostly in the x-direction, i.e., in the direction of axonemal length; random motion in the y-direction was clearly reduced by the poly-lysine coating of the glass surface. In the latter two cases, amino-type polystyrene beads (see Materials and Methods) were used to prevent direct attachment of the beads with the glass surface. Sample: *Anthocidaris crassispina*. Temperature: 28°C.

vibration period (as can be seen in curves $I_x$–$I_x$ and $II_x$–$II_x$ in Fig. 5). This analysis, like an FFT analysis, is thus useful for detecting the time constant of a given movement. When two microbeads vibrate at the same frequency but with a certain phase difference, their cross-correlation function will also become a periodic wave. In such a case, however, the peak position will be at $0 + d, p + d, 2p + d, \ldots$, where d is the phase difference. We found that this relationship holds for the movements of a single vibrating bead in x- and y-directions, as shown by $I_x$–$I_y$, $II_x$–$II_y$ in Fig. 5. The phase difference *d* varied with beads, indicating that the direction of the regular vibration differed from one bead to another in those experiments in which glass surfaces were not coated with poly-lysine.

The movements of two microbeads attached to the same axoneme, however, were found to vibrate exactly in phase in the x-direction. Two microbeads attached to the same axoneme vibrated at the same frequency in ~80% of the cases in which vibration was detectable. In other instances, one of the two beads showed no vibration, or beat at a frequency different from that of the other. We were surprised to find that whenever the two beads beat at the same frequency, the cross-correlation function between their movements in the x-direction was almost identical with the autocorrelation function of the movement of each bead, not only in period but also in phase (compare $I_x$–$I_x$ with $I_x$–$II_x$, and $II_x$–$II_x$ with $II_x$–$III_x$ in Fig. 5). The cross-correlation between two vibrating microbeads in 18 cases, in which the distance between two beads ranged from 4.7 to 41 μm, indicated that the phase difference in vibration should be less than the time

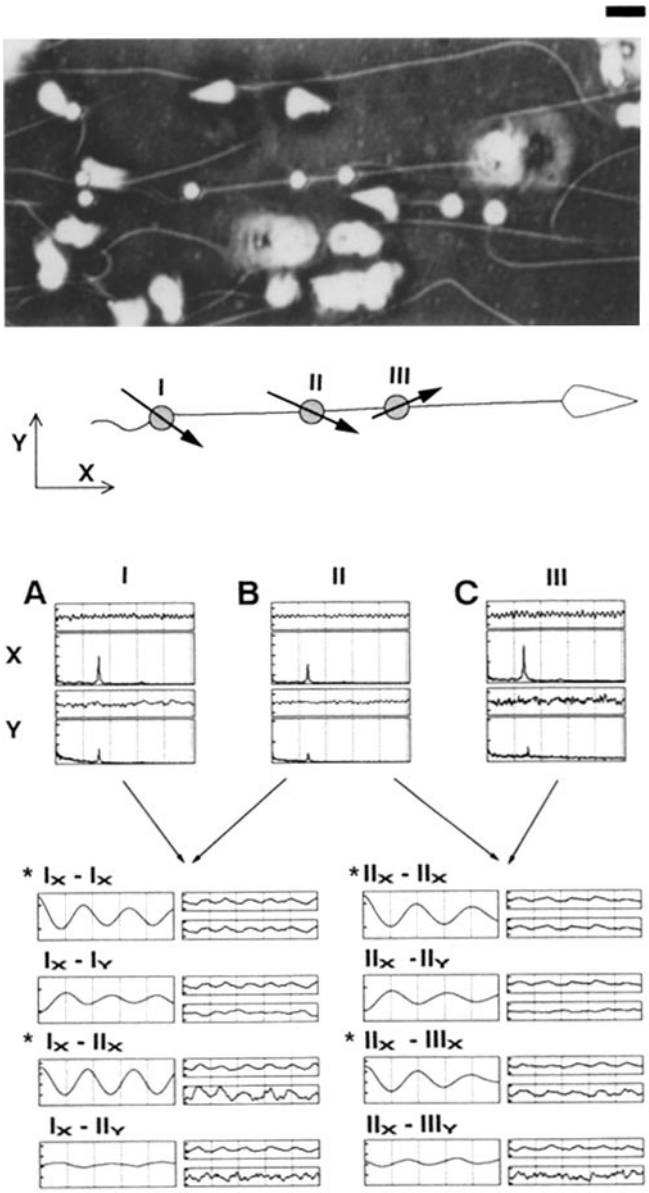


*Figure 5.* Correlation between movements of two microbeads attached to the same axoneme. The photograph and the illustration show the axoneme analyzed. The arrows indicate the directions of motion of each microbead revealed by the following analyses. *A–C* show the motion of microbeads I, II and III (labeled in the illustration), respectively. The x- (*upper*) and y-outputs (*lower*) are shown with respective FFT spectra as in Figs. 7 and 8 (with the same horizontal scales). The vertical scales are in 5 nm (outputs) and 1 nm (FFT spectra). The lower eight figures are the results of correlation analyses. For examples, $I_x$-$I_x$ indicates the autocorrelation of motion of the microbead I in the longitudinal direction, and $II_x$–$III_y$ indicates the cross-correlation between the longitudinal motion of the microbead II and the lateral motion of the microbead III. The figures on the left side are the auto- or cross-correlation functions, averaged from ten calculations using 1,024 data points sampled at 50 kHz. The vertical scale is a relative value; the horizontal full scale is 20 ms. Shown on the right side are part of the pair of data used (vertical scale, 5 nm; the horizontal scale, 4 ms [full scale = 20 ms]). The correlation functions marked by * represent instances when the two motions are correlated almost exactly in phase. Sample: *Hemicentrotus pulcherrimus.* Temperature: 20°C. Bar, 5 μm.

resolution of our apparatus, 1 ms. This result indicates that an entire outer doublet moves virtually uniformly in the x-direction in a vibrating axoneme.

These findings indicate that, in agreement with the conclusion from the observation on axonemes firmly attached to the glass surface, the direction of vibration is predominantly longitudinal. It is most likely that the vibration is due to a back-and-forth shearing motion between two groups of the outer doublets, one group adhering to the glass surface and the other moving together with the microbead (see Discussion).

### *Vibration Amplitudes*

The axonemal microtubules can be thus regarded as stiff rods that move in unison in the longitudinal direction. Hence the vibration amplitude measured with suppressed Brownian movement should directly reflect the shearing length between microtubules. Some of these axonemes (~40%) vibrated with significantly larger amplitudes than those observed previously without using poly-lysine coat for unknown reasons. Examinations of these larger amplitudes revealed a striking feature: the amplitudes assumed stepwise values reflecting the size of tubulin.

Figs. 6 *A*, 7 *A*, and 8 *A* show regular vibrational motions in the longitudinal direction in three examples. We analyzed 150,000–200,000 data points for each, sampled at 10 kHz for 15–20 s. Fig. 6 shows an example in which the vibration seems sinusoidal, i.e., forward and backward movements were symmetrical. This pattern of vibration was observed in ~60% of ~100 specimens where the vibration was detected. The histograms for the amplitudes of motion in both ascending and descending phase have the same Gaussian distributions with value of 4.6 ± 1.1 nm (Fig. 6, *B* and *C*). The amplitude was always <8 nm. The period of this vibration was 2.9 ± 0.3 ms (Fig. 6 *D*), i.e., the mean frequency was 345 Hz. In this example, the two phases in the vibration wave, ascending and descending, were symmetrical and cannot be distinguished by amplitudes (Fig. 6, *B* and *C*), periods (Fig. 6 *D*) or the plot of amplitudes vs periods (Fig. 6, *E* and *F*). This means that the shearing motion was almost symmetric in both directions. It could then be described by $D = 2.3 \times \sin(2.2 \times T)$, where $D$ and $T$ are the shear distance (nm) and time (ms). The maximal velocity is calculated to be ~5.0 μm/s; this is 1/2 to 1/3 of the sliding velocity estimated in beating axonemes.

Fig. 7 shows an example of an asymmetric waveform, the ascending phase being faster than the descending phase. About 30% of the microbeads that underwent vibration displayed this pattern. In the ascending phase, the amplitudes were distributed around a single value of 12.3 nm (Fig. 7 *B*). In the descending phase, on the other hand, the amplitudes were distributed near two discrete peak values of 4.1 and 12.1 nm (Fig. 7 *C*): the difference between the two peak amplitudes was ~8 nm, the size of a tubulin dimer. In relation to the occurrence of the two peak values, it is interesting to note that the movement in the descending phase often seemed stepwise, owing to the presence of small shoulders (Fig. 7 *A*; *lower figure*). This step may reflect the cause for the occurrence of two peaks in the amplitude histogram. The periods displayed a single, narrow distribution around ~4 ms, with a small subpeak at ~3 ms (Fig. 7 *D*). The maximal

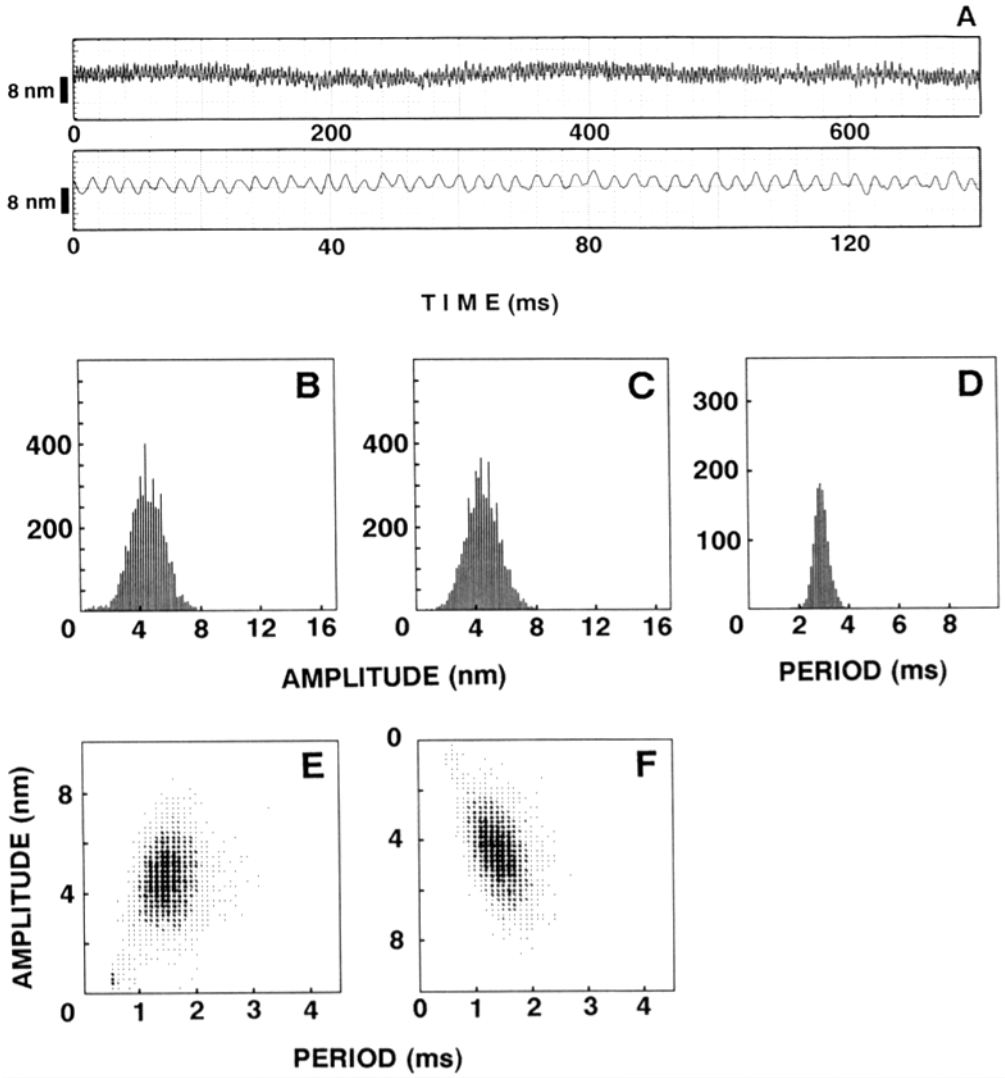


*Figure 6.* Statistical analysis of the vibration shown in Fig. 4 *C*. (*A*) Vibration curve shown in two different time scales Same as in Fig. 4 *C*. (*B*) Histogram of peak-to-peak amplitudes from each bottom to the next peak, i.e., the amplitude of the ascending phase. The averaged amplitude is 4.6 ± 1.1 nm ($n$ = 5,087). (*C*) Histogram of peak-to-peak amplitude from each peak to the next bottom, i.e., the amplitude of the describing phase. The averaged amplitude is 4.6 ± 1.1 nm ($n$ = 5,036). (*D*) Histogram of the interval between top-peaks. The averaged period is 2.9 ± 0.3 ms ($n$ = 5,093). (*E*) Relationship between peak-to-peak amplitude and period of the ascending phase. (*F*) Relationship between peak-to-peak amplitude and period of descending phase. A total of 150,000 points were sampled at 10 kHz.

rate of the ascending and descending phases (amplitude/period) are ~10 and ~5 μm/s, respectively (Fig. 7, *E* and *F*). Analyses on different examples indicated that there was no consistent relationship between the asymmetry of vibration and the proximal-distal polarity of the axonemes.

Fig. 8 shows another example where the amplitudes were unusually large. Patterns similar to this were observed in ~10% of the microbeads that underwent vibration. The histogram of the peak-to-peak amplitudes shows four distinct peaks at 10.9, 19.8, 27.3 and 36.2 nm in the ascending phase (Fig. 8 *B*), and five peaks at 3.7, 10.8, 19.6, 27.7 and 36.7 nm in the descending phase (Fig. 8 *C*). The differences between these peak amplitude values are all close to 8 nm, the size of the tubulin dimer. In the ascending phase no peak was detected around 4 nm (Fig. 8 *B*). Despite the occurrence of such discrete amplitudes, the vibration periods did not assume clear discrete values but were distributed around a broad peak at ~6.5 ms (Fig. 8 *D*). The rates of shearing both in the ascending and descending phases were almost constantly ~10 μm/s (Fig. 8, *E* and *F*). Thus, in all of these three cases, the shearing rate was comparable with the rate of microtubule sliding observed in disintegrating axonemes.

## Discussion

### *High-frequency Vibration as Back-and-forth Shearing between Two Groups of Outer Doublets*

Two independent experiments using a two-dimensional detector have established that the high-frequency vibration occurs primarily in longitudinal (x) direction. In the first experiment, we monitored movements in axonemes firmly attached to a poly-lysine–coated glass surface. In those axonemes whose random motion was suppressed, the vibration occurred only in the x-direction. The second experiment analyzed the cross-correlation between motions of two microbeads attached to the same axoneme. In all of the 18 cases that displayed a single vibration frequency, the movements of two microbeads were synchronized exactly in phase. This observation indicates that the high-frequency vibration does not involve propagation of minute bends but is a back-and-forth shearing of entire lengths of microtubules. If the movement involved bend propagation, the microbead motion should have differed in phase depending on their positions. Thus the high-frequency vibration differs

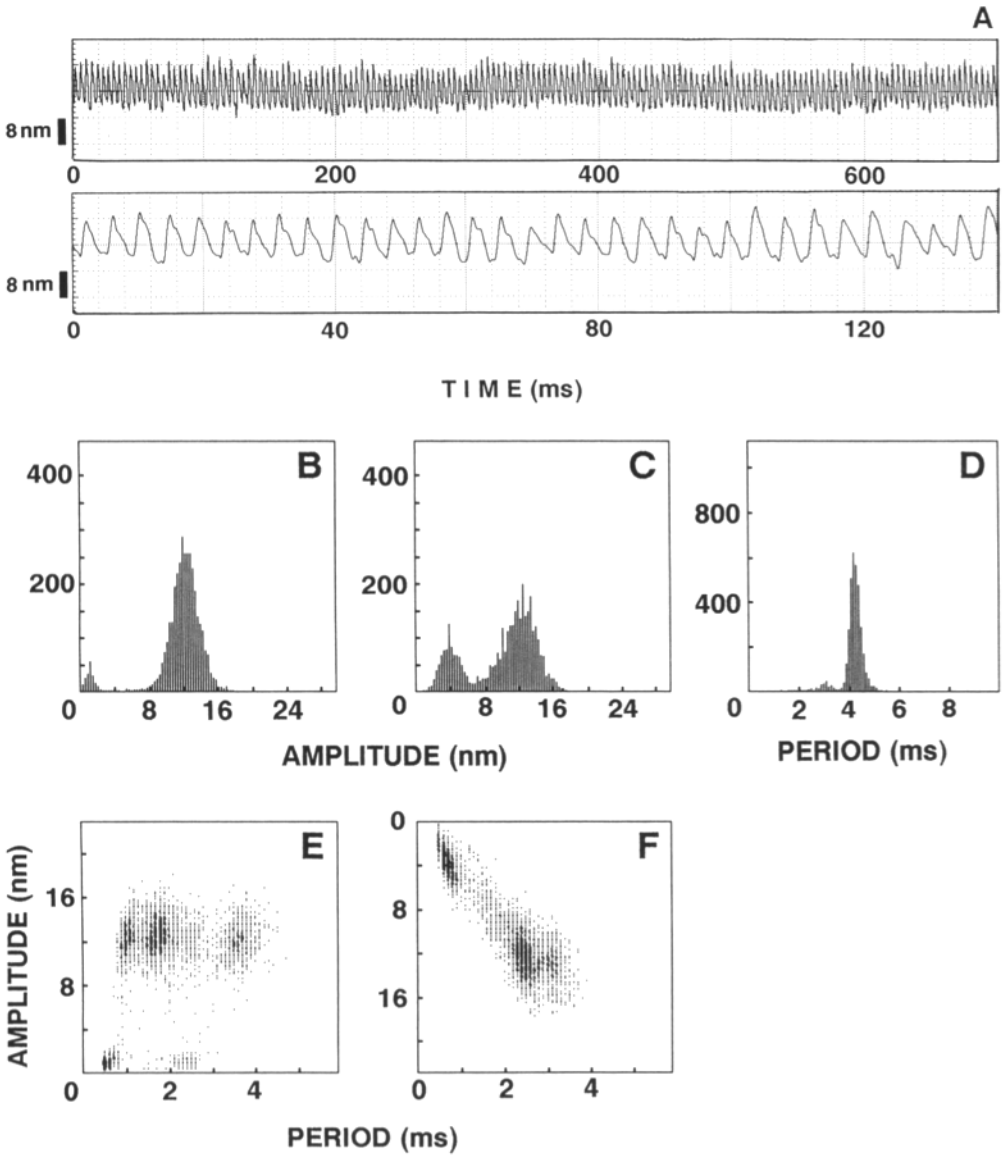


*Figure 7.* Statistical analysis on another type of vibration observed with axonemes firmly attached to poly-lysine–coated glass surface. Figures are arranged as in Fig. 6. In Fig. 7 *B*, a small peak appearing at ~1.5 nm is an artifact caused by noises near the level of sampling threshold. The main peak has an average of 12.3 ± 1.6 nm ($n$ = 3,330). In the descending phase (*C*), on the other hand, the amplitudes were distributed around two discrete peaks with averaged values of 4.1 ± 1.1 ($n$ = 883) and 12.1 ± 2.0 nm ($n$ = 2,631).

from the ordinary axonemal movement in which a wave of curvature propagates from base to tip. This observation indicates that change in curvature is not a prerequisite for the generation of vibration.

The observation that two different microbeads on the same axoneme always beat in unison indicates also that the movement at a given moment is due to an active shear between a pair of outer doublets only, out of nine possible pairs; if multiple pairs caused the movement simultaneously, the movement of two beads, which were not necessarily attached on the same outer doublet, would often have differed in phase. In those rare cases when two microbeads displayed two different vibration frequencies, or when a single bead displayed two discrete frequencies (Kamimura and Kamiya, 1989), sliding might have been taking place between two or more pairs of outer doublets independently. Analyses on such rare cases will be reported elsewhere.

Why active shearing movement mostly occurred only between one pair of outer doublets is not understood. There may be particular pairs of outer doublets wherein dynein arms are activated more easily than in other pairs. Alternatively, under our experimental conditions, an active interaction of dynein arms with the adjacent outer doublet may occur so rarely that the probability of simultaneous activation of two or more pairs may be very low. This interpretation is possible since we typically observed the high frequency vibration with only 1/5–1/3 of the total microbeads attached to the axonemes.

### *Amplitude and Frequency of Axonemal Vibration*

As we have reported previously (Kamimura and Kamiya, 1989), the concentration of ATP and vanadate, a potent dynein inhibitor, affected the frequency or amplitude of vibration. However, the amplitude and frequency varied more or less independently; reduction in ATP concentration decreased the frequency with little effect on the amplitude, whereas vanadate and NEM decreased the amplitude without affecting the frequency.

The amplitude appears to reflect the number of active dynein arms, as long as it does not exceed 8 nm (for the cases when it exceeds 8 nm, see below), since it is lowered by inhibitors that decrease the number of active dynein arms; vanadate has been known to be a dynein inhibitor that brings

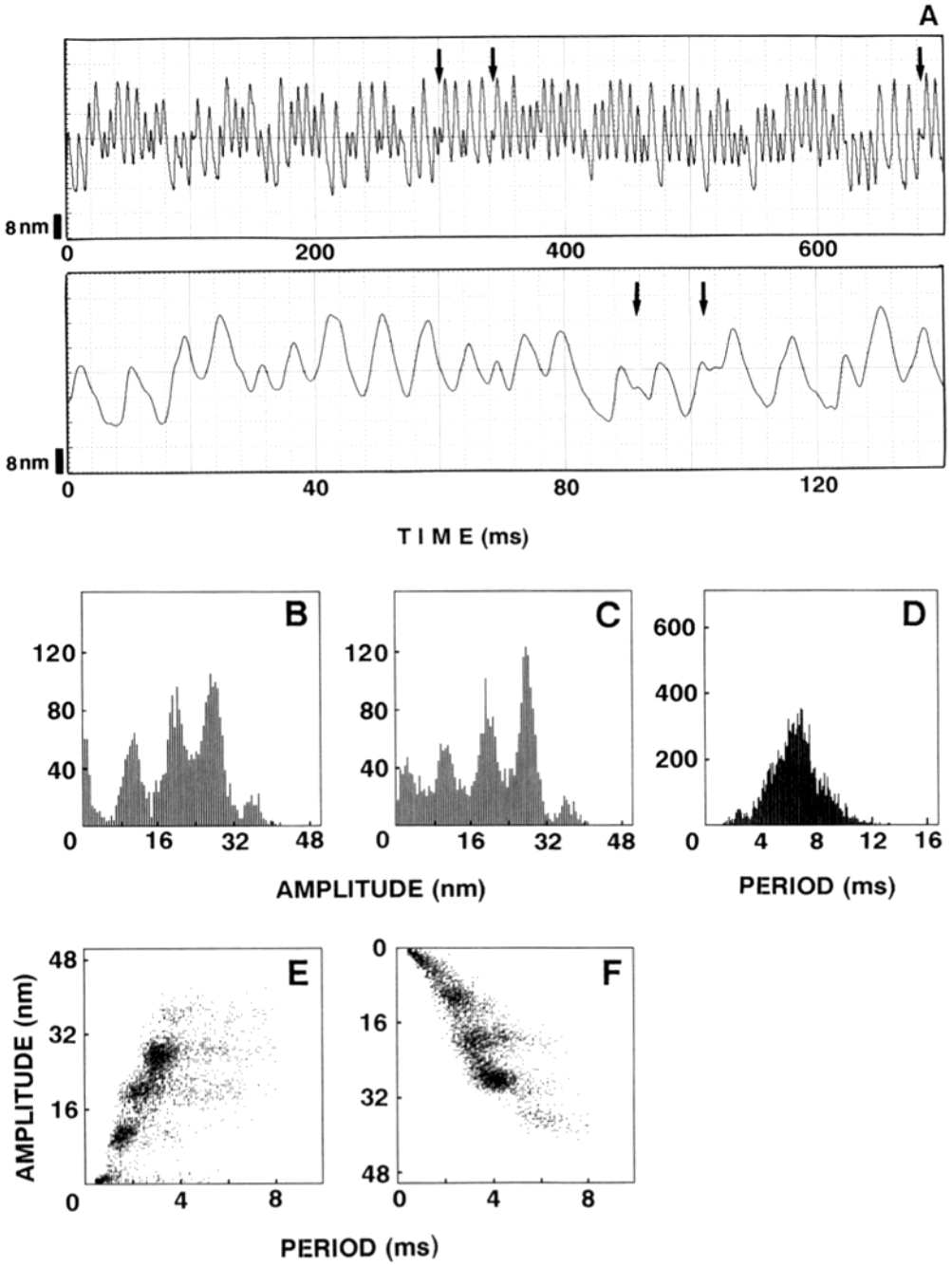


*Figure 8.* Statistical analysis of the vibration shown in Fig. 4 *D*. Figures are arranged as in Figs. 6 and 7. Arrows in *A* indicate instances when movement with a 4-nm amplitude appears. For explanations for each figure see Fig. 6 legend. A total of 200,000 points were used for analysis. The distinct peaks are at 10.9 ± 2.0 nm ($n$ = 601), 19.8 ± 1.6 nm ($n$ = 769), 27.3 ± 1.8 nm ($n$ = 1,031) and 36.2 ± 1.3 nm ($n$ = 140) in the ascending phase (*B*), and at 3.7 ± 1.8 nm ($n$ = 418), 10.8 ± 1.6 nm ($n$ = 408), 19.6 ± 1.8 nm ($n$ = 767), 27.7 ± 1.8 nm ($n$ = 1,023) and 36.7 ± 1.6 nm ($n$ = 131) in the descending phase (*C*).

dynein to a kinetical dead end (Shimizu and Johnson, 1983), a state in which dynein binds to outer doublets only very weakly (Vale et al., 1989). Probably NEM also reduces the number of active dynein by irreversibly inactivating it. The vibration amplitude may therefore reflect the force produced by the total dynein arms that interact with outer doublets. It may be that the amplitude is determined by the balance between the active force and an elastic load due to deformation of internal components of axoneme, such as inter-doublet links. If this is true, the axoneme displaying high frequency vibration must be considered to be working against a large internal elastic load. Such an internal elastic load may be present in intact axonemes, but not in protease-treated axonemes.

On the other hand the dependency of the vibration frequency upon ATP concentration is similar to that of the sliding velocity of microtubules in disintegrating axonemes, or of the beat frequency in reactivated axonemes. All show Michaelis-Menten type dependence with an apparent Km for MgATP of ~100 $\mu$M, a value more than 50 times higher than the Km observed in ATP hydrolysis by dynein (Johnson, 1985). The reason why the microtubule sliding rate decreases at low ATP concentrations is not totally clear. However, it is possible that a small fraction of dynein arms devoid of ATP and ADP are present at low ATP concentrations, and that these arms impede microtubule sliding through their strong interactions with the outer doublet. The effect of lowered ATP concentration, then, differs from the effect of vanadate which does not promote strong interaction between dynein and outer doublets.

The MgATP concentration dependence of sliding velocity or of flagellar beat frequency differs from that of the force generated by sliding microtubules (Kamimura and Takahashi, 1981). Oiwa and Takahashi (1988) have measured the force produced by outer doublets in sea urchin axonemes at various MgATP concentrations, and found that the maximal force developed was almost constant over a concentration range of 3.5–350 $\mu$M. If these properties hold true also in the present system, where microtubules slide only in a nanometer range, the observation that the vibration amplitude did not vary with ATP concentrations is consistent with the above idea that the amplitude is determined by the force developed by dynein arms. If lower ATP concentrations decrease the sliding velocity while leaving the vibration amplitude constant, the vibration frequency would naturally decrease.

### *Four and Eight Nanometer Steps in Microtubule Shearing*

The present study revealed that the vibration amplitude reflects the size of tubulin monomer and dimer. In view of the finding that microtubules in vibrating axonemes behave like stiff rods, we may expect that a high resolution recording of the microtubule movement will reveal steps of the size of tubulin, since the locations of different dynein arms relative to the tubulin with which they interact are identical along the axonemal length.

The mode of vibration varied depending on whether or not its amplitude exceeded 8 nm. In the majority of cases, the vibration curve was sinusoidal with peak-to-peak amplitudes ranging between 0 and 8 nm, as shown in Fig. 6. The average amplitude was typically ~4 nm, i.e., the size of the tubulin monomer (Fig. 6, *B* and *C*). In experiments using polylysine-coated glass, however, the vibration sometimes had amplitude >8 nm. Analyses of amplitude in such cases revealed a novel feature: the peak-to-peak amplitudes tended to take stepwise values that can be expressed as

$$A = 8 \times N + 4 \text{ nm},$$

where $N$ is an integer ($\geqslant 0$ or $\geqslant 1$, depending on the direction of shear. Fig. 7 and 8). The amplitude steps thus reflect the molecular size of tubulin monomer and dimer. The occurrence of such discrete values of amplitude could be explained by an assumption that the dynein arm has a tendency to start sliding at a tubulin subunit of one type (e.g., alpha tubulin) and stop at the other type (e.g., beta tubulin) in the same or other tubulin dimer that is located closer to the minus-end of the same protofilament (Fig. 9).

It is important to note that the occurrence of discrete amplitudes does not necessarily mean that dynein arms have a tendency to slide stepwise: it only means that the amplitude of the sliding is limited by certain discrete lengths. Therefore, the molecular basis for the occurrence of stepwise amplitudes could be either in the mechanism for sliding itself or in the mechanism that regulates the microtubule sliding in axonemes.

### *Mechanism for the High-frequency Vibration: a Model*

As we have seen above, the high frequency vibration appears to occur as a shearing movement between a single pair of microtubules in a given moment. In order for a vibration to occur, there must be antagonizing forces that alternate. Both of them can be active forces produced by dynein-microtubule interaction. Alternatively, only shear in one direction is caused by an active force and the other by a passive, elastic force. The symmetrical vibration profile in the majority of cases as shown in Fig. 6, however, suggests that both of the two counteracting forces must be active, produced by different pairs of outer doublets. The mechanism that causes the switching between the two different active pairs should be of key importance for the understanding of the high frequency vibration. Although the present study has not established the mechanism for the switching, it has narrowed the possibilities. First, as we have seen above, curvature is not involved in this switching. Second, since vanadate and NEM decreased the amplitude to a level below the tubulin size while leaving the frequency constant, the absolute shear length may not be important either.

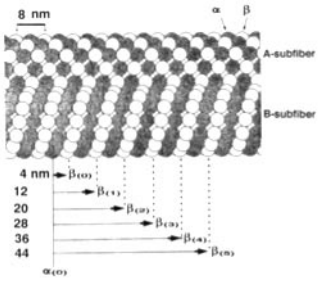


*Figure 9.* A model explaining occurrence of the stepwise amplitudes. A dynein arm starts sliding at one type of a tubulin monomer, e.g., alpha tubulin (0), to the other type of monomer (in this case beta tubulin) that is positioned in the minus direction on the same protofilament. If the dynein stops at the Nth beta tubulin, the sliding amplitude will be $4 + 8 \times N$ (nm). Since other dynein arms are located with a periodicity of multiples of the size of the tubulin dimer, all dynein arms along the length of the doublet should be under identical conditions with respect to their relative distance to alpha and beta tubulin.

These considerations have led us to a model that will serve as a working hypothesis for future studies. We speculate that each phase, ascending or descending, of a particular vibration cycle is produced by a subfraction of dynein arms on one outer doublet. The subfraction of dynein arms are in a particular state of ATPase cycle such that they can actively interact with the adjacent microtubule. The dynein arms would then produce force and slide until their energy level lowers to a critical point. We now assume that (*a*) the axoneme contains an elastic component whose tension increases steeply when stretched up to 4 nm; (*b*) the cessation of force production is accelerated by the tensile force received by each dynein, i.e., the mechanical deformation of each dynein; and (*c*) at the ATP concentrations used in the present study, the subpopulation of dynein arms that produce force are dissociated from the adjacent outer doublet immediately after the cessation of their force production. The cessation of force production can then be a cooperative process; when some of the dynein arms stop producing force and detach from the microtubule, other dynein arms still producing force will receive more tension, which will then promote the cessation of force production. The dynein arms detached from the adjacent outer doublet hydrolyze ATP relatively slowly (compared to the vibration frequency), at a rate constant of 100–120/s (Shimizu et al., 1989), and it is only some time after the hydrolysis that they can produce the force necessary for oscillation again. The next cycle of vibration is driven by other subpopulation of dynein arms that have not been engaged in force production in the previous cycle. Thus, ac-

cording to our model, the vibration frequency does not represent the ATP turnover rate itself, but reflects the mean duration of force production by each dynein molecule.

With the above assumptions, outer doublets within the axoneme are expected to oscillate since an active shear in one direction will be followed by a movement in the opposite direction caused by an internal elastic force. However, such a mechanism may produce an asymmetric vibration in which only the movement in one direction is ATP dependent. The curve of displacement vs. time will become a saw-tooth type. Thus, although these assumptions may be enough to explain some asymmetric vibrations such as those shown in Fig. 7, these are not enough to explain the occurrence of symmetric vibration shown in Fig. 6. This example probably resulted from two antagonizing forces produced by identical mechanisms. In such a case, dynein arms on two opposite rows must alternate in producing force. The mechanism that causes this alteration is difficult to imagine, but it may be that a passive shearing movement of doublets caused by elastic force triggers the active movement in the same direction. Alternatively, dynein may have a difficulty to interact with microtubules that are moving in the direction opposite to the direction of the force it generates.

We need more assumptions to explain the stepwise distribution of vibration amplitudes. We speculate that the axoneme contains two kinds of elastic components in parallel: a stiffer one working in the range of 0–4 nm, and the other, more elastic one, working in the range of the order of 10 nm. We assume further that the former (stiffer) elastic unit may be a microtubule-associated protein that can be displaced to the adjacent tubulin dimer (and thus move for the lengths of multiple of 8 nm) when appropriate force is applied. Some dynein subspecies may serve as this component. The latter, more elastic, component may correspond to the so-called interdoublet link or "nexin" link. The stepwise distribution of amplitude can then be explained by assuming different contributions from the two elastic components. The occasional appearance of steps in the vibration curve (Fig. 7 *A*) may be due to transient, weak association of the dislocatable elastic element with tubulin. We propose that the complicated distribution of amplitudes in Fig. 8 reflects the complicated properties of the overall elastic force, which affects the probability of the cessation of force production by dynein.

The above model is admittedly based on several assumptions that have little experimental support at present. It is to be examined whether the axoneme has two types of components that restrict the vibration amplitude. In an attempt to evaluate the contribution of elastic components to the vibration, we observed axonemes after briefly treating them with elastase; we found that the vibration amplitude increased as the model predicts (unpublished results). This supports the hypothesis that there are elastic component(s) that restrict the vibration amplitude. Although our model does not specify what conditions favor the occurrence of amplitude >8 nm, it is conceivable that some unknown mechanism regulates the behavior of the presumptive elastic components.

It also remains to be investigated whether the cessation of force production is accelerated by mechanical stress on dynein. This possibility has been supported by observations that dynein–microtubule interaction becomes unstable when dynein exerts large tension. In measurements of force produced by sliding outer doublets using fine elastic glass needles, Takahashi and Kamimura (1983) and Oiwa and Takahashi (1988) have often experienced oscillation of the outer doublet bundles; the oscillation tended to occur as the developed force reached some critical values (Kamimura, S., unpublished observation). If the cessation of force production by dynein is actually accelerated by the tension it produces (and receives), dynein should be considered to be equipped with a mechanical switch that constitutes a feedback loop needed for oscillation. Dynein may be a mechano-chemical oscillator in itself.

## *Conclusion*

We have shown that an analogue apparatus based on a quadrant photodiode and a sensitive amplifier can detect displacement of microbeads in two dimensions with a precision of subnanometer, and demonstrated that the outer doublet in flagellar axonemes undergoes a minute back-and-forth vibration at a frequency as high as 300 Hz. The vibration amplitude has been found to reflect the size of tubulin. Thus, this technique has offered an opportunity to look at the dynein–microtubule interaction at the level of a single tubulin with a high time resolution. The oscillatory movement raises the possibility that dynein has an intrinsic nature to oscillate when subjected to tension. Further analyses of the vibration should give us insights into the functional properties of dynein as well as the molecular mechanism of the flagellar and ciliary motility. Application of our technique to other motile systems would also be of great interest. The recent development in video microscopy has provided another means to detect subnanometer particle displacement, and has already revealed novel features in biological movements (Gelles et al., 1988). The time resolution of a video-based method, however, is usually limited to 1/60 s or so. Detection of nanometer-scale displacements at higher time resolution as used in this study may reveal still more striking features in many biological phenomena.

We thank Drs. Fumio Oosawa (Aichi University of Technology), Eckhard Mandelkow, and Peter Rehse (Max-Planck-Institute, Hamburg) for their critical reading of the manuscript and for valuable discussions.

This study has been supported by grants-in-aid from the Ministry of Education, Science and Culture of Japan (01657001, 02239101, 03223101).

Received for publication 29 August 1991 and in revised form 9 December 1991.

### *References*

Brokaw, C. J. 1967. Adenosine triphosphate usage by flagella. *Science (Wash. DC)*. 156:76–78.

Brokaw, C. J. 1982. Models for oscillation and bend propagation by flagella. *In* Symposia of the Society for Experimental Biology XXXV, Prokaryotic and Eukaryotic Flagella. Amos, W. B., and J. G. Duckett, editors. Cambridge University Press, Cambridge. 313–338.

Brokaw, C. J. 1990. Flagellar oscillation - New vibes from beads. *J. Cell Sci.* 95:527–530.

Gelles, J., B. J. Schnapp, M. P. Sheetz. 1988. Tracking kinesin-driven movements with nanometre-scale precision. *Nature (Lond.)*. 331:450–453.

Gibbons, I. R. 1981. Cilia and flagella of eukaryotes. *J. Cell Biol.* 91:107s–124s.

Gibbons, B. H., and I. R. Gibbons. 1972. Flagellar movement and adenosine triphosphatase activity in sea urchin sperm extracted with Triton X-100. *J. Cell Biol.* 54:337–357.

Gibbons, B. H., and I. R. Gibbons. 1974. Properties of flagellar "rigor waves" formed by abrupt removal of adenosine triphosphate from actively swimming sea urchin sperm. *J. Cell Biol.* 63:970–985.

Gibbons, I. R., M. K. Cosson, J. A. Evans, B. H. Gibbons, B. Houck, K. H.

Martinson, W. S. Sale, and W.-J. Y. Tang. 1978. Potent inhibition of dynein adenosinetriphosphatase and of the motility of cilia and sperm flagella by vanadate. *Proc. Natl. Acad. Sci. USA.* 75:2220–2224.

Gibbons, I. R., J. A. Evans, and B. H. Gibbons. 1982. Acetate anions stabilize the latency of dynein 1 ATPase and increase the velocity of tubule sliding in reactivated sperm flagella. *Cell Motil.* 1:181–184.

Gibbons, B. H., W.-T. J. Tang, and I. R. Gibbons. 1985. Organic anions stabilize the reactivated motility of sperm flagella and the latency of dynein 1 ATPase activity. *J. Cell Biol.* 101:1281–1287.

Johnson, K. A. 1985. Pathway of the microtubule-dynein ATPase and the structure of dynein: A comparison with myosin. *Annu. Rev. Biophys. Biophys. Chem.* 14:161–188.

Kamimura, S. 1987. Direct measurement of nanometric displacement under an optical microscope. *Appl. Optics.* 26:3425–3427.

Kamimura, S., and R. Kamiya. 1989. High-frequency, nanometre-scale vibration in 'quiescent' flagellar axonemes. *Nature (Lond.).* 340:476–478.

Kamimura, S., and K. Takahashi. 1981. Direct measurement of the force of microtubule sliding in flagella. *Nature (Lond.).* 293:566–568.

Kobayashi, T., T. Martensen, J. Nath, and M. Flavin. 1978. Inhibition of dynein ATPase by vanadate and its possible use as a probe for the role of dynein in cytoplasmic motility. *Biochem. Biophys. Acta* 16:146–154.

Oiwa, K., and K. Takahashi. 1988. The force-velocity relationship for microtubule sliding in demembranated sperm flagella of the sea urchin. *Cell Struct. Func.* 13:193–205.

Okuno, M., and Y. Hiramoto. 1979. Direct measurements of the stiffness of echinoderm sperm flagella. *J. Exp. Biol.* 79:235–243.

Shimizu, T., and K. A. Johnson. 1983. Presteady state kinetic analysis of vanadate-induced inhibition of the dynein ATPase. *J. Biol. Chem.* 258: 13833–13840.

Shimizu, T., and I. Kimura. 1974. Effects of N-ethylmaleimide on dynein adenosine triphosphatase activity and its recombining ability with outer fibers. *J. Biochem.* 76:1001–1008.

Shimizu, T., S. P. Marchese-Ragona, and K. A. Johnson. 1989. Activation of the dynein adenosinetriphosphatase by cross-linking to microtubules. *Biochemistry.* 28:7016–7021.

Takahashi, K., C. Shingyoji, and S. Kamimura. 1982. Microtubule sliding in reactivated flagella. *In* Symposia of the Society for Experimental Biology XXXV, Prokaryotic and Eukaryotic Flagella. Amos, W. B., and J. G. Duckett, editors. Cambridge University Press, Cambridge. 159–177.

Takahashi, K., and S. Kamimura. 1983. Dynamic aspects of microtubule sliding in sperm flagella. *J. Submicrosc. Cytol.* 15:1–3.

Vale, R. D., D. R. Soll, and I. R. Gibbons. 1989. One-dimensional diffusion of microtubules bound to flagellar dynein. *Cell.* 59:915–925.

Yano, Y., and T. Miki-Noumura. 1980. Sliding velocity between outer doublet microtubules of sea urchin sperm axonemes. *J. Cell Sci.* 44:169–186.